DOI: 10.13009/EUCASS2023-756
Aerospace Europe Conference 2023 – 10TH EUCASS – 9TH CEAS

Shell models of turbulence in aero-optics

Albina Tropina
Texas A&M University
3141 TAMU, College Station, TX, US, 77843
atropina@tamu.edu

Abstract

This paper presents a model, which is based on the combination of the shell model of turbulence and aero-optics for the case of the buoyancy driven turbulence and turbulence in the vibrationally non-equilibrium flow. It is shown that the refractive index spectrum generated using the shell model reflects experimentally observed structure functions of temperature. Analysis of the fluctuating part of the refractive index for the vibrationally non-equilibrium flow has been performed. Changes in the spectrum and irradiance profiles are controlled by the rate of dissipation of the temperature variance, which depends on the level of the vibrational non-equilibrium.

1. Introduction

The effects of turbulence have been studied for a long period of time and much progress has been made, but many phenomena associated with turbulence are still difficult to predict, especially for large Reynolds numbers. One such phenomenon is the laser beam propagation through atmospheric turbulence. At high Reynolds numbers, aero-optical effects cause beam spreading and attenuation[1-3]. The aero-optical effects are connected with the turbulent pulsations of the temperature, pressure and humidity and they strongly affect performance of laser beam systems[4-5]. We can analyze properties of aero-optical distortions in the Fourier space by introducing a spectrum of the refractive index[6]. Tatarskii in his classical book[7] has formulated an analytical theory of aero-optical effects based on a statistical description of turbulence leading to predicted amplitude and phase fluctuations of the propagating electromagnetic wave. It was shown that scattering of electromagnetic wave in a turbulent atmosphere and refractive index fluctuations for isotropic turbulence follow a -11/3 law in the inertial subrange. To characterize the refractive index fluctuation spectrum we need to know both the kinetic energy and temperature cascade behaviour.

For the considered range of Reynolds numbers, methods based on Direct Numerical Simulations (DNS) still cannot resolve the dissipative subrange of the spectrum. As an alternative, statistical properties of isotropic and homogeneous turbulence have been studied using shell models of turbulence. The basic idea of any shell model is a transition from the physical space to the Fourier space. The next step is a construction of the discrete set of shells and an appropriate choice of the interaction and coupling between neighboring shells to take into account the main properties of the original Navier-Stokes (NS) equations. Finally, the formed system of non-linear differential equations describing the time evolution of amplitudes of the velocity pulsations can be solved numerically using standard methods for stiff equations. The most comprehensive review of properties of shell models related to the turbulent kinetic energy cascade is presented in a paper by Biferale[8]. Depending on the chosen nonlinear coupling the shell model can preserve the total energy and volume in a phase space as in the Desnyansky and Novikov model[9] or additionally preserve the total helicity as in the Gletzer-Okhitani-Yamada (GOY) shell model[10,11] and in its improved version Sabra shell model[12]. A generalization of the helical shell models is presented in the paper by Benzi et al[13], where the authors used a helical decomposition of the Navier-Stokes equations in the Fourier space. Despite the evident disadvantage of shell models, such as an absence of any space geometry factors, most of the shell models reproduce the Kolmogorov's turbulence scaling and some of them[10-12] show intermittency behavior. It worth noting that the shell intermittency is a temporal intermittency in contrast to the spatial intermittency in a real three-dimensional turbulent flow[14,15].

Another class of shell models has been used to study the temperature spectrum in a turbulent flow. Depending on the Rayleigh or the Richardson number, temperature can be the passive or active scalar. In the former case at low Ri numbers, a temperature spectrum can be formally obtained using shell models for passive scalars[16-18]. The resulting shell equation describes the time evolution of a scalar field (temperature amplitude θ) which is passively carried by the fluid flow down to high wavenumbers where the energy is dissipated due to viscosity. The shell model for the passive scalar additionally to the conservation of energy and volume in the absence of forcing, viscosity and diffusivity must conserve a variable $\frac{1}{2}\sum_k \theta_k^2$, which reflects a conservation of entropy. It was shown, that for Prandtl numbers $Pr = \frac{\nu}{D} \geq 1$ there is the inertial convective subrange in the temperature spectrum E_θ, which coincides with the Obukhov-Corrsin law[19,20] $E_\theta = C_\theta \chi \varepsilon^{-1/3} k^{-5/3}$, where k is the wavenumber, $C_\theta \cong 0.68$ is the Obukhov-Corrsin constant, χ is the scalar dissipation rate and ε is the energy dissipation rate.

DOI: 10.13009/EUCASS2023-756

For turbulent convection caused by the buoyancy force, which is one of the main sources of the temperature fluctuations in the atmosphere, the system of NS equations additionally includes the buoyancy term in the Boussinesq approximation. It is important for shell models because an effect of compressibility and changes in density are connected only with the changes of temperature, when incompressibility condition $div\vec{v} = 0$ is still valid. In the Fourier space it transforms to the relation $\vec{u}(k) \cdot \vec{k} = 0$, thus the Fourier amplitude of the velocity $\vec{u}(k)$ is perpendicular to $\vec{k}$. As a result, NS equations being projected onto a plane perpendicular to $\vec{k}$ in the Fourier space, allows us to remove the pressure term.

Changes in the scaling exponent observed in the highly stratified atmosphere and transition from the Kolmogorov scaling to the Bolgiano-Obukhov (BO) scaling due to the effects of the buoyancy forces, were initially explained by Bolgiano and Obukhov[21,22]. The buoyancy force provides forcing at all length scales and as a result in the buoyancy subrange temperature fluctuations are scaled as $k^{-7/5}$ compared with $k^{-5/3}$ in the Kolmogorov scaling. Shell models for the buoyancy-driven stratified turbulence were introduced by Brandenburg [23] and Suzuki et al [24]. A dual scaling effect was discussed in the paper by Ching[16] in the frame of the Brandenburg shell model, which can be considered as a modification of the Desnyansky and Novikov model[9] by the inclusion of the buoyancy term. In this shell model, nonlinear terms in the equation for the velocity pulsations include both the direct kinetic energy transfer to smaller scales and the inverse transfer from the smaller scales to the larger scales. The main conclusion is that the BO scaling is closely connected with the inverse transfer of the kinetic energy. For the case of the weak stratification the model shows, that the temperature behaves like a passive scalar and being modified[24] can capture intermittency effects.

In the more recent publication[25] the authors explored the applicability of shell models based on complex variables (GOY based shell models) and the Brandenburg shell model to study the confined Rayleigh–Taylor turbulent convection. It was shown that the dual BO and Kolmogorov scaling depends on the buoyancy force and this effect is better reproduced by the Brandenburg shell model. Furthermore, for the study of confined turbulent convection the scale of the geometrical confinement determines the Bolgiano length scale, which is usually defined by matching the fluxes of the viscous dissipation rate from both scaling regimes.

The goal of this paper is to understand the effect of the buoyancy driven turbulence and turbulence in the vibrationally non-equilibrium flow on aero-optical disturbances. The model has been developed to study the refractive index spectrum behaviour and optical distortions of the laser beam, propagating in atmosphere. The model is used for the analysis of the refractive index structure parameter C_n^2. The C_n^2 parameter is based on the 2/3-law for the structure function[7] and characterizes the strength of turbulence in aero-optics.

2. Formulation of the problem

Using the Oberbeck-Boussinecq approach, when changes in density are included only in the gas state equation, but not in the continuity equation, the main system of equations for a buoyancy driven flow and flow in the vibrational non-equilibrium has the form (1)-(3)

$$\rho_0 \left(\frac{\partial \vec{v}}{\partial t} + (\vec{v} \cdot \nabla)\vec{v}\right) = -\nabla P + \mu \Delta \vec{v} + \rho_0 g \alpha \theta \vec{k}, \quad (1)$$

$$c_p \rho_0 \left(\frac{\partial T}{\partial t} + (\vec{v} \cdot \nabla)T\right) = \lambda \Delta T + \rho_0 \frac{\varepsilon - \varepsilon^*(T)}{\tau_{VT}}, \quad (2)$$

$$\rho_0 \left(\frac{\partial \varepsilon}{\partial t} + (\vec{v} \cdot \nabla)\varepsilon\right) = \lambda_V' \Delta \varepsilon - \rho_0 \frac{\varepsilon - \varepsilon^*(T)}{\tau_{VT}}, \quad (3)$$

where $P = p - \rho_0 g z$, $\lambda_V' = \lambda_V \frac{\partial T_V}{\partial \varepsilon}$, τ_{VT} is the vibrational-translational relaxation time, $\varepsilon, \varepsilon^*, T_v$ are the vibrational energy, equilibrium vibrational energy and vibrational temperature, respectively, g is the acceleration due to gravity, λ_V is the vibrational thermal conductivity, the α, ν,χ are the volume expansion coefficient, kinematic viscosity and thermal conductivity of the gas, respectively.

Two problems are considered such as a) flow generated by the buoyancy force (equations (1-2), without the last term in the eq.(2)) and b) the vibrationally non-equilibrium flow (eq.(1)-(3)).

It is clear, that buoyancy force can cause anisotropy of the flow, but as was shown in [26], stably stratified flows at low Richardson numbers and turbulent flows in the regime of Rayleigh–Bénard convection are nearly isotropic. Thus, for the inertial range of isotropic homogeneous turbulence, the Kolmogorov's hypothesis of the energy spectrum independence of fluid properties is still valid. The formal procedure for the derivation of any shell model includes the Fourier transform of the Navier-Stokes equations to the wave space and shell averaging, which results in the system of equations (4)-(6) for Fourier amplitudes of the velocity $u^2(t,k) = \left\langle \sum_{\frac{k}{\sqrt{2}} \le |k'| \le \sqrt{2}k} v_j(t, \overrightarrow{k'}) v_j(t, -\overrightarrow{k'}) \right\rangle$, the Fourier components of the translational temperature $\theta_n = \theta(k,t)$ and vibrational energy $\varepsilon_n = \varepsilon(k,t)$.

DOI: 10.13009/EUCASS2023-756

$$\frac{\partial\, \boldsymbol{u(k,t)}}{\partial t} = k\left(u^2\,(k-1,t) - 2u(k,t)u(k+1,t)\right) - \frac{1}{Re}k^2u(k,t) + Ri\,\theta(k,t), \quad (4)$$

$$\frac{\partial \boldsymbol{\theta}(k,t)}{\partial \boldsymbol{t}} = k\big(u(k-1,t)\theta(k-1,t) - 2u(k,t)\theta(k+1,t)\big) - \frac{1}{Re\,Pr}k^2\theta + \beta u_n + R_{vib}\big(\theta(k,t)\theta(k,t) - \varepsilon(k,t)\theta(k,t)\big), \quad (5)$$

$$\frac{\partial \boldsymbol{\varepsilon}(\boldsymbol{k},\boldsymbol{t})}{\partial t} = k(u(k-1,t)\varepsilon(k-1,t) - 2u(k,t)\varepsilon(k+1,t) - A_{vib}k^2\theta(k,t) - R_{vib}\big(\theta(k,t)\theta(k,t) - \varepsilon(k,t)\theta(k,t)\big), \quad (6)$$

where $v_j(t,\vec{k})$ is the Fourier components of the velocity, wavenumbers $k_i = k_0 h^i$, i=0,1,….N-1, h=2 is the distance between shells, N is the total number of shells , k_0 is the wavenumber corresponding to the largest scale,

$Ri = \frac{g\alpha\Delta T l_0}{v_0^2}$ is the Richardson number, $R_{vib} = \frac{\Delta\varepsilon}{c_{p0}(T_s - T_0)}$ is the parameter, which characterises the level of the vibrational non-equilibrium, $A_{vib} = \frac{\lambda_v}{v_0 l_0 \rho_0}$ is the parameter which characterizes diffusivity of the vibrational energy. The non-linear convective terms in eq. (4)-(6) includes only the nearest neighbour shell interactions as in the dyadic shell model. The last term in eq. (5),(6) is the proposed closure for the vibrational-translational energy exchange term.

The next step is the transition to aero-optics, the refractive index spectrum and the refractive index structure parameter C_n^2 [7]. By definition the second order structure function D_n of the refractive index is the mean-square average of the refractive index measured at two points separated by the distance R. Introducing the outer scale L as the size of the largest turbulent eddies in the flow and the inner scale l_0, the structure function D_n of the refractive index, is related to the refractive index structure parameter C_n^2 as follows

$$D_n(x+R,x) = \langle[n(x+R) - n(x)]^2\rangle = C_n^2 R^{\frac{2}{3}} \quad l_0 \le R \le L \quad and \quad (7)$$

$$D_n(x+R,x) = \langle[n(x+R) - n(x)]^2\rangle = C_n^2 R^2 l_0^{-4/3} \quad 0 \le R \le l_0\ . \quad (8)$$

The inner scale of turbulence l_0 is the size of the smallest inhomogeneities in the temperature distribution, and it is the intercept point of two asymptotes of the temperature structure function in the viscous-diffusive and inertial range of the temperature spectrum[7]. For air the inner scale is $l_0 = \left(\frac{27\cdot C_\theta \Gamma(\frac{1}{3})}{5\cdot Pr}\right)^{3/4} \eta \cong 7.4\,\eta$, where $\eta = \left(\frac{\nu^3}{\varepsilon}\right)^{1/4}$ is the Kolmogorov's scale. The refractive index is $n = 1 + K_{GD}\frac{p}{RT}$, where K_{GD} is the Gladstone-Dale (GD) constant. In a general case, K_{GD} is not constant due to the polarizability dependence on the translational and vibrational temperature. This effect is important for the analysis of the interferometry results in the hypersonic flow [27-29]. Following the standard procedure $p = \bar{p} + p', T = \bar{T} + T', K_{GD} = \bar{K}_{GD} + K'_{GD}$, $n = \bar{n} + n'$, where $\bar{p}, \bar{T}, \bar{K}_{GD}$, $\bar{n}$ and p', T', K'_{GD}, n' are the mean and fluctuating parts of the pressure, temperature, Gladstone-Dale constant and refractive index. Assuming that $\frac{T'}{\bar{T}} \ll 1$ the fluctuating part of the refractive index has a form

$$n' \cong \bar{K}_{GD}\left(-\frac{\bar{p}T'}{R\bar{T}^2} + \frac{p'}{R\bar{T}} - \frac{p'T'}{R\bar{T}^2}\right) + \frac{\bar{p}}{R\bar{T}}\left(K'_{GD} - \frac{K'_{GD}T'}{\bar{T}} + \frac{K'_{GD}p'}{\bar{p}} - \frac{K'_{GD}p'T'}{\bar{T}}\right).$$

Neglecting by the second and third order terms, the final expression for the fluctuating part of the refractive index is as follows

$$n' \cong \bar{K}_{GD}^2\left(-\frac{\bar{p}T'}{R\bar{T}^2} + \frac{p'}{R\bar{T}}\right) + \frac{\bar{p}K'_{GD}}{R\bar{T}}, \quad (9)$$

A three-dimensional spectrum $\Phi(\vec{k})$ of any scalar field is a Fourier transform of the correlation function $B(\vec{r})$, i.e.

$$\Phi(\vec{k}) = \frac{1}{(2\pi)^3}\int B(\vec{r})\exp(-i\vec{r}\cdot k)\,d\vec{r}, \quad (10)$$

where $\vec{r} = \bar{r}_1 - \bar{r}_2$ is the displacement vector, and the correlation function for the refractive index is $B_n(\bar{r}_1 - \bar{r}_2) = \overline{n'(\bar{r}_1)n'(\bar{r}_2)}$. Using relations (9),(10), the general formula for the refractive index spectrum in the vibrationally non-equilibrium flow is

DOI: 10.13009/EUCASS2023-756

$$\Phi_n(\vec{k}) = \frac{\bar{K}_{GD}^2}{R^2\bar{T}^2}\left[\Phi_p(\bar{k}) + \frac{\bar{p}^2\Phi_T(\bar{k})}{\bar{T}^2} - \frac{2\bar{p}Re(\Phi_{Tp}(\vec{k})}{\bar{T}} + \frac{\bar{p}^2\Phi_{KK}(\bar{k})}{\bar{K}_{GD}^2} - \frac{2\mathrm{Re}(\Phi_{KT}(\bar{k}))\bar{p}^2}{\bar{K}_{GD}\bar{T}} + \frac{2\mathrm{Re}(\Phi_{Kp}(\bar{k}))\bar{p}}{\bar{K}_{GD}}\right], \quad (11)$$

where $\Phi_p(\bar{k}), \Phi_T(\bar{k}), \Phi_{KK}(\bar{k})$ are pressure, temperature, and K_{GD} constant spectra. Additional terms include Φ_{Tp}, Φ_{KT} and Φ_{Kp}, which are the temperature-pressure, K_{GD} constant –temperature and K_{GD} constant-pressure co-spectra, respectively.

In this paper the dependence of the Gladstone-Dale constant on the vibrational temperature and the pressure contribution to the refractive index fluctuations are neglected compared with the temperature spectrum contribution [30,31]. Thus, the refractive index spectrum depends only on the temperature spectrum, which is taken from the shell model (4)-(6) a) for the flow generated by the buoyancy force and b) for the vibrationally non-equilibrium flow. The dimensionless refractive index parameter C_n^2 is found from the relation for the refractive index spectrum in the inertial subrange $\Phi_n^*(k) = C_n^{2*}k_*^{-\frac{11}{3}}$, which follows $k_*^{-\frac{11}{3}}$ dependence. When the mean temperature gradient in the vertical direction $\beta = abs\left(\frac{dT}{dz}\right) \neq 0$ is not small, and buoyancy feeds the kinetic energy, to provide adequate forcing eq. (5) includes the term proportional to β. In this case changes in the C_n^{2*} parameter are controlled by the mean temperature gradient β. Dividing the turbulent layer into sub-layers with a constant temperature gradient gives C_n^{2*} dependence on the coordinate.

2. Numerical results and analysis

The system of equations (4)-(6) is stiff due to a wide range of time scales covering the inertial and viscous intervals of the spectrum. To obtain an accurate estimation of the energy and temperature spectrum at the steady case the code was running several times with different total time and time steps until the average results coincided. Input parameters include $k_0 = \frac{1}{L}$, which is inversely proportional to the integral length scale, and values of $u_0, \theta_0, \varepsilon_0$ at the first shell. Additional dimensionless parameter $\tilde{E}_v = \frac{\varepsilon_0}{E_{total\_0}}$ describes the initial level of the vibrational non-equilibrium in the first shell. Calculations were run at parameters typical for air, thus kinematic viscosity, thermal diffusivity and thermal expansion coefficients were taken at atmospheric pressure as $\nu = 1.6 \cdot 10^{-5}\frac{m^2}{s}$; $\chi = \frac{\lambda}{\rho c_p} = 22.2 \cdot 10^{-6}\ \frac{m^2}{s}$; $\alpha = 3.4 \cdot 10^{-3}K^{-1}, Re = 10^6, N = 25, k_0 = 0.0628, u_0 = 1$.

First, the results for the flow generated by the buoyancy force are presented. Figure 1 shows the refractive index spectrum calculated using the shell model (4)-(5), the Tatarskii model [7] for the inertial subrange and von Karman model. For the latter, the refractive index spectrum is

$$\Phi_n(k) = 0.033C_n^2\exp\left(-\frac{k^2}{k_m^2}\right)/(k^2 + k_0^2)^{11/6}, \quad (12)$$

and $k_0 = \frac{2\pi}{L}$; $k_m = \frac{5.92}{l_0}$, inner scale $l_0 = 4.27 \cdot 10^{-5}m$. It is seen that the shell model predicts the behavior of the spectrum in the inertial and dissipative subranges, and it is in a good agreement with the von Karman model, which is often used in aero-optics.

DOI: 10.13009/EUCASS2023-756

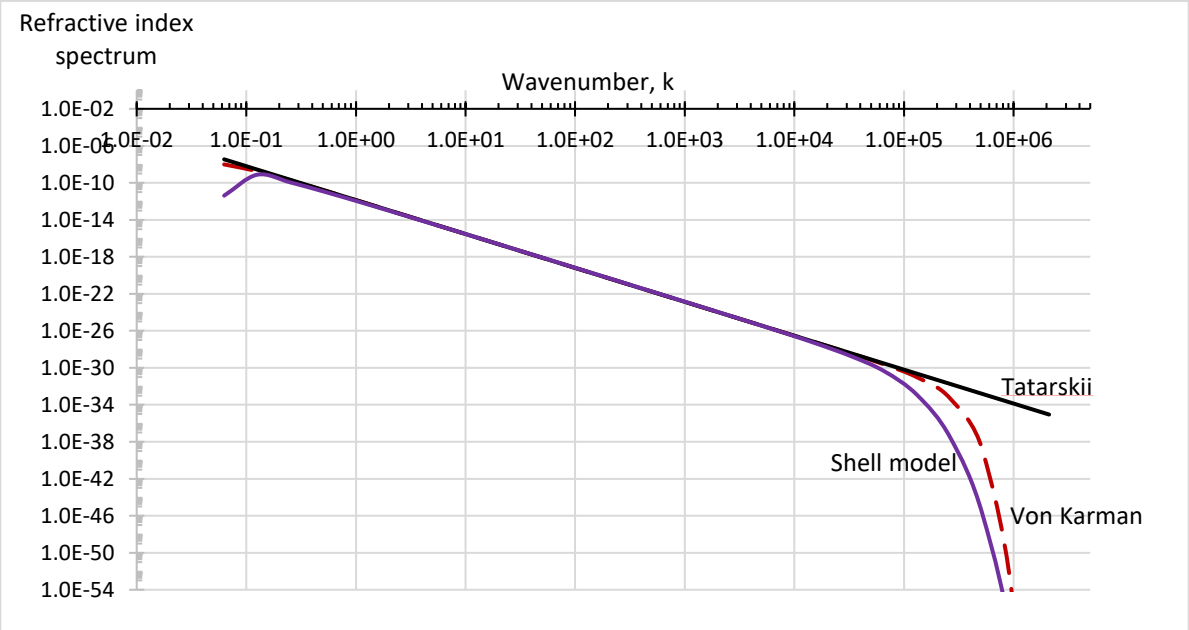

Figure 1: Refractive index spectrum

Changes in the structure function parameter C_n^{2*} depending on the temperature gradient are shown in Fig.2. The range of C_n^{2*} varies in limits 10^{-16} to 10^{-11} with the increase of C_n^{2*} with the increase of β, which reflects the enhancement in the turbulence strength with the increase of the temperature gradient.

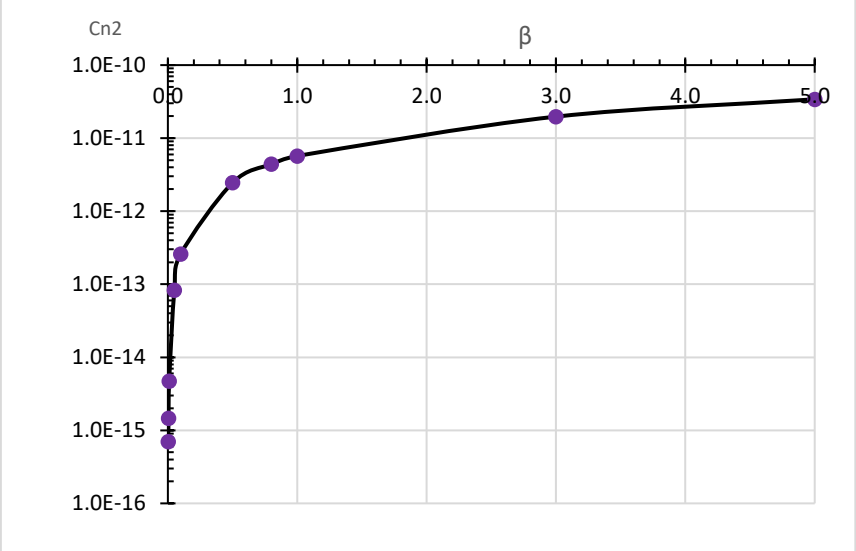

Figure 2: The structure function parameter as a function of the temperature gradient β.

To understand the behavior of C_n^{2*} as a function of the temperature gradient β an additional analysis of the dissipation rates of the kinetic energy of turbulence, the rate of dissipation of the temperature variance and structure functions of temperature is carried out. The dissipation rate of the kinetic energy of turbulence is $\varepsilon = 2\nu\langle(\nabla v)^2\rangle$, which in the shell model equals to $= \nu \sum_{n=1}^{n=N} k_n^2 u_n^2$. The dissipation rate of the temperature variance is $\varepsilon_\theta = 2\chi\langle(\nabla T)^2\rangle$ and in the shell model it is defined as $\varepsilon_\theta = \chi \sum_{n=1}^{n=N} k_n^2 \theta_n^2$. Figure 3 shows dependence of ε and ε_θ on the temperature gradient. After comparison of results in Fig.2-3 it is clear, that the dependence of the structure function parameter on the temperature gradient follows the same tendency as the dissipation rate of the temperature variance, thus the enhancement of the temperature dissipation rate at the high temperature gradient causes the increase of the structure function parameter.

DOI: 10.13009/EUCASS2023-756

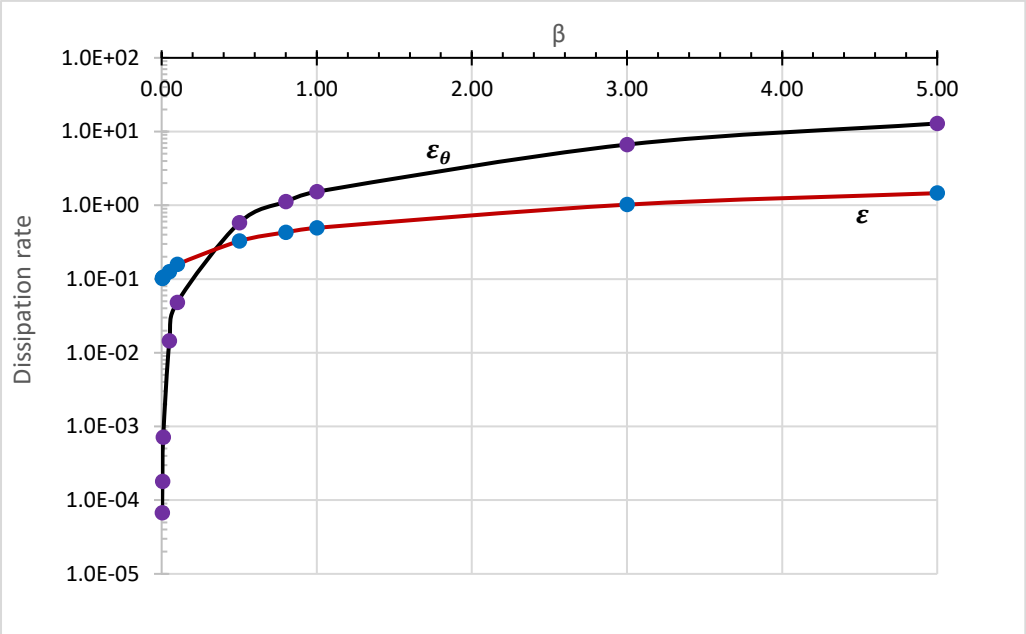

Figure 3: Dissipation rate of the kinetic energy and temperature variance as a function of β

Going back to the standard definition of C_n^2 given by (7) the behavior of the structure functions of the refractive index and accordingly the structure functions of temperature must follow the $R^{\frac{2}{3}}$ law in the inertial subrange. The second order structure functions of velocity and temperature in the shell model can be defined as follows

$$D_v(k_n) = \langle [u_n]^2 \rangle; \quad D_\theta(k_n) = \langle [\theta_n]^2 \rangle. \tag{13}$$

Figure 4 shows dependence of the structure functions of temperature on the wavenumber at the various temperature gradient β. The black line in Fig.4 represents the classical scaling in the inertial subrange of the spectrum, which is proportional to $k^{-2/3}$.

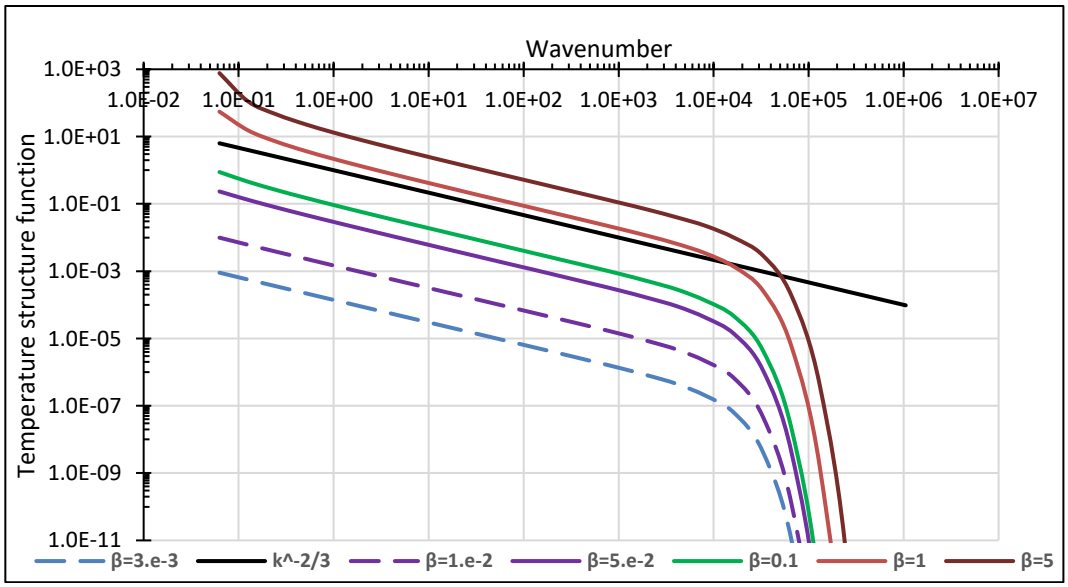

Figure 4: Structure functions of temperature as functions of the temperature gradient β

It is seen that the structure functions of temperature follow the same slope corresponding to classical scaling in the inertial subrange of the spectrum, and values of the structure functions are changed depending on C_n^{2*}, which in turn changes depending on the temperature gradient. It is noteworthy that because of non-dimensional units in shell models, the relations are scaled with some empirical constant. But having one value of C_n^2 at the specific temperature gradient

DOI: 10.13009/EUCASS2023-756

the temperature gradient in the model can be adjusted as follows. Changes in the C_n^{2*} values are closely related to the temperature variance dissipation rate $\bar{N} = \chi\overline{\left(\frac{\partial T'}{\partial z}\right)^2}$ (in the shell model $\varepsilon_\theta = \chi\sum_{i=1}^{N} k_i^2\theta_i^2$) showing $\varepsilon_k^{-1/3}\varepsilon_\theta k^{-5/3}$ scaling for the fluctuation spectrum of temperature. In the shell model at the fixed Reynold number ε_θ is controlled by the value of θ_0 in the first shell. Using the measured temperature dissipation rates from [32] and Eq.(14) for the temperature variance dissipation rate $\bar{N}$, the values of θ_0 in the first shell depending on the temperature variance dissipation rate ε_θ can be defined.

$$\bar{N} = -\frac{\partial}{\partial z}(\bar{T}\overline{\omega' T'}) + \beta(\bar{\omega}\bar{T}) + \beta(\overline{\omega' T'}) = \kappa_t\frac{\partial \bar{T}}{\partial z} + \beta(\bar{\omega}\bar{T}) + \beta(\overline{\omega' T'}). \quad (14)$$

This dependence is shown in the insert in Fig.5. Using this profile of θ_0 the refractive index structure parameter C_n^2 as a function of the height (Fig.5) is calculated and compared with the experimental data from [35]. It is seen that the model yields good agreement with the experimental data from the ground level through the troposphere ($\leq 13\ km$). Summarizing all the above, shell models can be used as a fast and computationally unexpensive tool for preliminary analysis and prediction of the main properties of aero-optical effects for thermal convective turbulence.

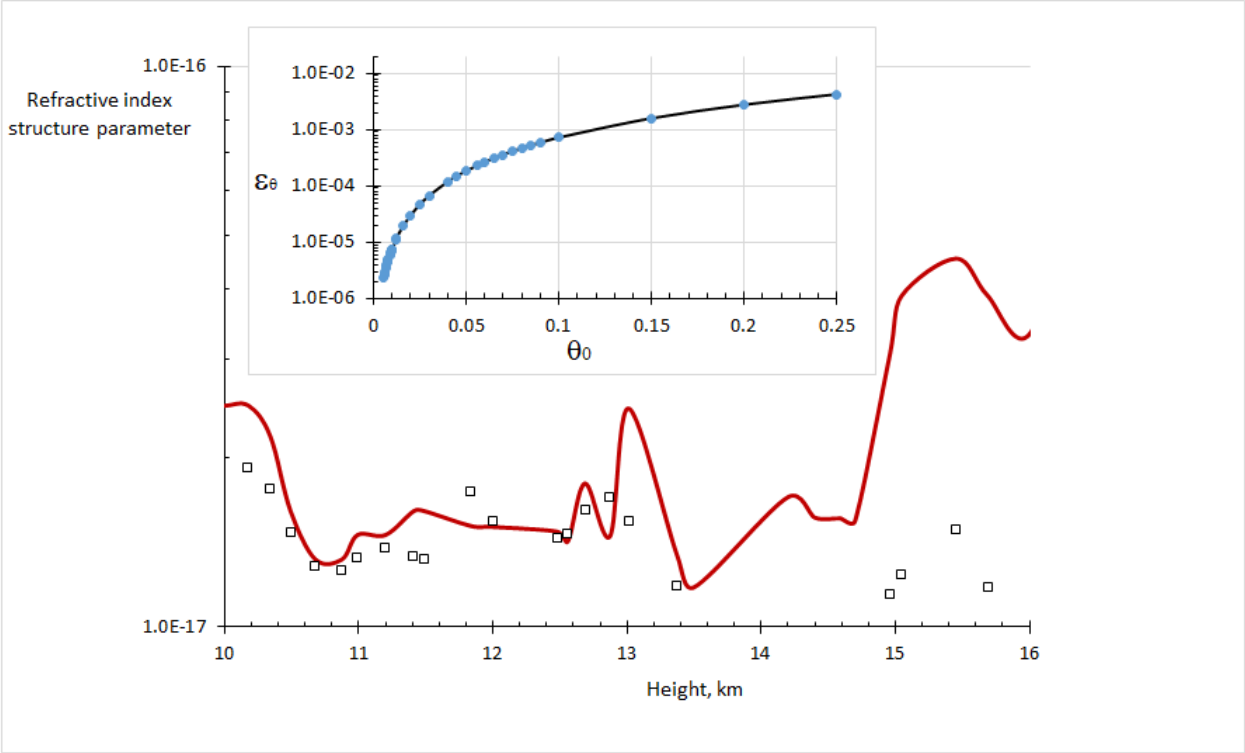

Figure 5: Refractive index structure parameter C_n^2 as a function of the height: red line- the calculation data, squares- the experimental data from [32]. Agreement is good up to ~13 km. The plot in the insert shows the dependence of the shell temperature variance dissipation rate on the values of θ_0 for the first shell.

For the vibrational non-equilibrium flow the temperature spectrum is controlled by two additional parameters such as R_{vib}, which defines the level of vibrational non-equilibrium of the flow and $\tilde{E}_v = \frac{\varepsilon_0}{E_{total\_0}}$, which describes the initial level of the vibrational non-equilibrium in the first shell. The temperature spectrum dependence on the parameter R_{vib} is shown in Fig.6. Straight lines in Fig.6 correspond to the classical Kolmogorov's scaling. It is seen that the effect of the vibrational non-equilibrium is more pronounced at the lower wave numbers (at large scales). The increase of R_{vib} causes the more postponed transition to the Kolmogorov's scaling regime. The parameter $\tilde{E}_v$ shows the similar effect but in the temporal development of the cascade. The more energy is in the vibrational mode in the first shell, the less is the local maximum of the energy dissipation rate considering that internal energy in the first shell is constant. With the increase of the level of the initial non-equilibrium the formation of the similarity regime moves to the later time. This qualitative analysis is effective for visualizing the physics of observed wave-front distortions, caused by the laser beam propagation through turbulence. The effect of the vibrational non-equilibrium can be easily captured in the beam irradiance profiles, which are constructed using the split step method and the temperature spectrum from (4)-(6)

DOI: 10.13009/EUCASS2023-756

as in [27]. Figure 7 shows the beam irradiance profiles for equilibrium case $\tilde{E}_v = 0$, and for two vibrationally non-equilibrium flows with the different initial level of the vibrational non-equilibrium in the first shell $\tilde{E}_v = 0.5; 1$. It is seen that the strength of the fluctuations in each case vary, showing the effect of the vibrational non-equilibrium on local focusing, refraction and diffraction of the beam, when light propagates through the turbulent region.

This analysis of the effects of the vibrational non-equilibrium on aero-optics using shell models is preliminary, and needs the additional study of effects associated with the inverse cascade, types of closure in (4)-(6)... etc. For example, previous analysis of the beam irradiance profiles in [27] showed that the magnitude of the beam irradiance changes with the inclusion of the "shell" intermittency effect.

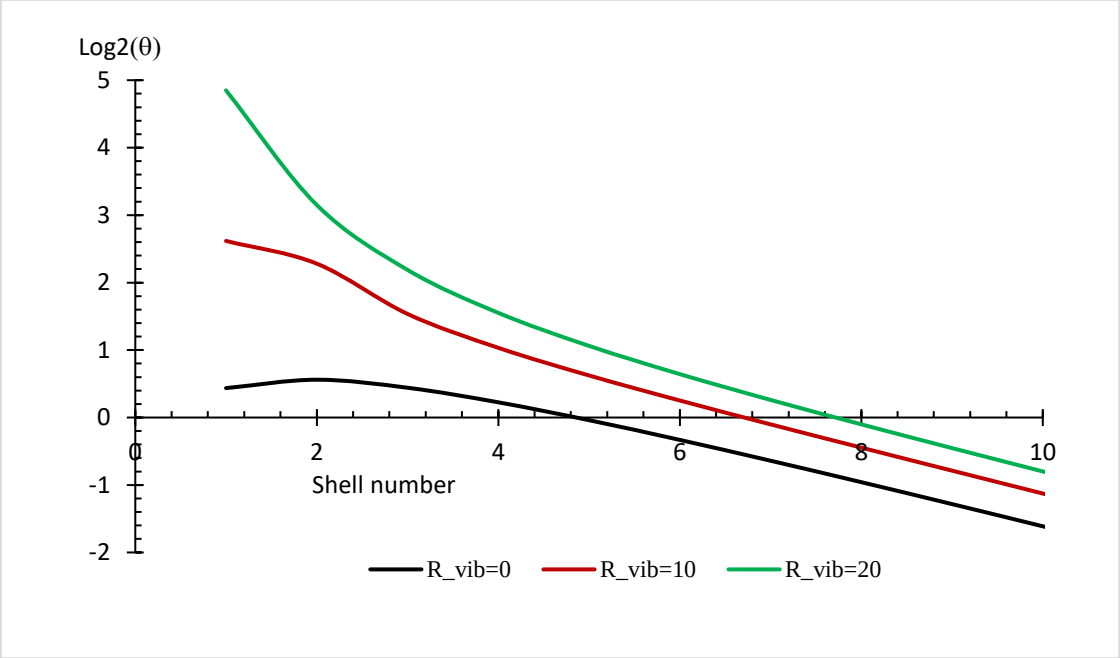

Figure 6: Temperature spectrum (steady state) as a function of R_vib

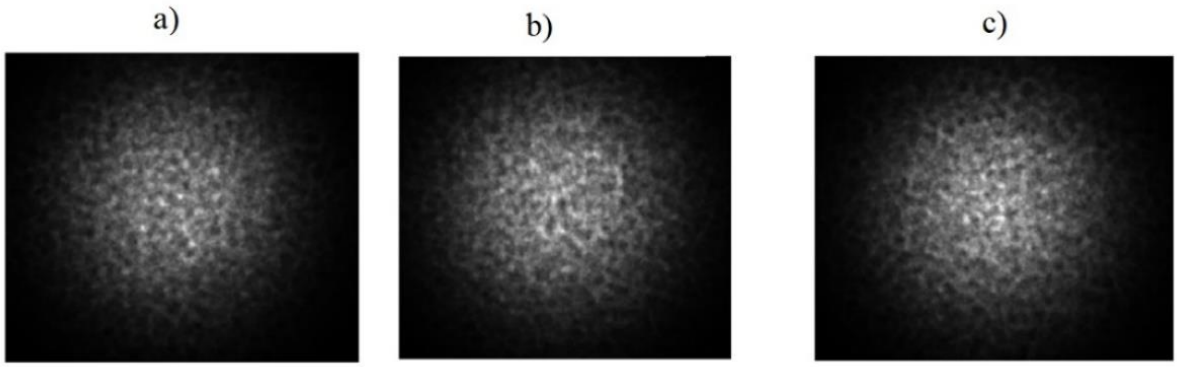

Figure 7: Beam irradiance profiles: a) $\tilde{E}_v = 0$, b) $\tilde{E}_v = 0.5$, c) $\tilde{E}_v = 1$.

Conclusions

A mathematical model, which combines a shell model of turbulence and aero-optics has been developed. The model is used to analyse behaviour of the refractive index spectrum and structure function parameter in thermal convective

DOI: 10.13009/EUCASS2023-756

turbulence and in the vibrationally non-equilibrium flow. The proposed approach agrees well with the observations of the refractive index, showing classical scaling in the inertial sub-range of the temperature and refractive index spectra. It is shown, that changes in the refractive structure parameter correlate well with the temperature variance dissipation rate, controlled by the initial values of temperature pulsations in the first shell. It is shown that the effect of the vibrational non-equilibrium is more pronounced at the lower wave numbers, and an increase of the vibrational non-equilibrium causes the more postponed transition to the Kolmogorov's scaling regime. Future work is needed to determine how the intermittency and inverse energy cascade, variations of the Gladstone-Dale constant in non-equilibrium flows, and different closures for the shell model affect aero-optics.

Acknowledgements

This work has been supported by internal funds of Texas A&M University.

References

[1] Kalensky, M., S. Gordeyev, and E.J. Jumper. 2019. In-Flight Studies of Aero-Optical Distortions Around AAOL-BC. *AIAA Aviation Forum.* AIAA Paper 2019-3253.
[2] Kemnetz, M., S. Gordeyev, S., and E.J. Jumper. 2019. Optical Investigation of a regularized shear layer for the examination of the aero-optical component of the jitter. *AIAA SciTech Forum.* AIAA Paper 2019-0469.
[3] Gordeyev, S., N. De Lucca, J. Morrida, E.J. Jumper, and D.J. Wittich. 2018. Conditional Studies of the Wake Dynamics of Hemispherical Turret Using PSP. *AIAA SciTech Forum.* AIAA Paper 2018-2048.
[4] Butler, L., M. Lozier, and S. Gordeyev. 2019. Effect of Varying Beam Diameter on Global Jitter of Laser Beam Passing Through Turbulent Flows. *AIAA Aviation Forum.* AIAA Paper 2019-3385.
[5] Sontag, J., M. Kemnetz, and S. Gordeyev. 2019. Spanwise Wavefront Analysis of Turbulence Amplification in a Turbulent Boundary Layer Forced by an External Shear Layer. *AIAA SciTech Forum.* AIAA Paper 2019-0054.
[6] Andrews, L.C. 1992. An analytical model for the refractive index power spectrum and its application to optical scintillations in the atmosphere. *Journal of Modern Optics.*39:1849-1853.
[7] Tatarskii, V.I. 1971. The effects of the turbulent atmosphere on wave propagation. NTIS, Springfield.
[8] Biferale, L. 2003. Shell models of energy cascade in turbulence. *Annual Rev. Fluid Mech*. 35:441-468.
[9] Desnyansky, V.N., and E.A. Novikov. 1974. The evolution of turbulence spectra to the similarity regime, *Izv. Akad. Nauk. SSSR Fiz. Atmos. Okeana*. 10:127-133.
[10] Gledzer, E.B., 1973. System of hydrodynamic type admitting two quadratic integrals of motion. Sov. Phys. Dokl. 18, 216-224.
[11] Ohkitani K. and M. Yamada. 1989. Temporal intermittency in the energy cascade process and local Lyapunov analysis in fully developed model of turbulence. *Prog. Theor. Phys*. 89:329-341.
[12] L'vov, V.S., E. Podivilov, A. Pomyalov, I. Procaccia and D. Vandembroucq. 1998. Improved shell model of turbulence. *Phys. Rev. E*. 58:1811-1822.
[13] Benzi, R., L. Biferale, R.M. Kerr and E. Trovatore. 1996. Helical-shell models for three-dimensional turbulence. *Phys. Rev. E*. 53:3541-3550.
[14] Benzi, R., L Biferale, S.Succi and F.Toschi. 1999. Intermittency and eddy viscosities in dynamical models of turbulence. *Physics of Fluids.*11:1221-1228.
[15] Mailybaev, A.A. 2021. Hidden scale invariance of intermittent turbulence in a shell model. *Physical review Fluids.* 6: 1-5.
[16] Ching, E.S. C. and W. C. Cheng. 2008. Anomalous scaling and refined similarity of an active scalar in a shell model of homogeneous turbulent convection. Ph*ysical review E*. 77:015303.
[17] Wirth, A., and L. Biferale. 1996. Anomalous scaling in random shell models for passive scalars. *Physical Review. E.* 54:4982.

DOI: 10.13009/EUCASS2023-756

[18] Jensen, M.H., G. Paladin and A. Vulpiani. 1992. Shell model for turbulent advection of passive-scalar fields. *Physical Review A*. 45:7214-7221.
[19] Obukhov, A.M. 1949. Structure of temperature field in turbulent flows. *Izv. Akad. Nauk SSSR Geophr. Geofiz*. 13:58-65.
[20] Corrsin, S. 1951. On the Spectrum of Isotropic Temperature Fluctuations in an Isotropic Turbulence. *J. Appl. Phys*. 22: 469-473.
[21] Bolgiano, R. 1959. Turbulent spectra in a stably stratified atmosphere. *J Geophys Res*. 64:2226-2229.
[22] Obukhov, A.M. 1959. Effect of Archimedean forces on the structure of the temperature field in a turbulent flow. *Dokl Akad Nauk SSSR*. 125:1246-1256.
[23] Brandenburg, A. 1992. Energy Spectra in a Model for Convective Turbulence. *Physical Review Letters.* 69:605-608.
[24] Suzuki, E., and S. Toh. 1995. Entropy cascade and temporal intermittency in a shell model for convective turbulence. *Phys Rev E*. 51:5628-5635.
[25] Li , L.,P. Liu, Y. Xing and H. Guo. 2020. Shell models for confined Rayleigh–Taylor turbulent convection. *Commun Nonlinear Sci Numer Simulat*. 84:105204.
[26] Verma, M., A. Kumar and A. Pandey. 2017. Phenomenology of buoyancy-driven turbulence: recent results. *New J. Phys*. 19: 025012.
[27] Hartman, D.V., A.A. Tropina and R.B. Miles. 2021. Numerical analysis and prediction of aero-optical effects, *AIAA SciTech Forum*. AIAA Paper 2021-0335.
[28] Tropina, A.A., Yue Wu, C.M. Limbach and R.B. Miles. 2020. Influence of vibrational non-equilibrium on the polarizability and refraction index in air: computational study. *Journal of Phys.D, Applied Physics*. 53:105201.
[29] Anaya, J., Tropina, A., Miles, R.B., Grover, M. 2023. Refractive index of diatomic species for nonequilibrium flows. *AIAA Aviation Forum.* AIAA Paper 2023-3478.
[30] Agg, R., J. Hill, S. F. Clifford, and R. S. Lawrence. 1980. Refractive-index and absorption fluctuations in the infrared caused by temperature, humidity, and pressure fluctuations. *J. Opt. Soc. Am.* 70:1192–1205.
[31] McBean, G.A., and J. Elliott. 1981.Pressure and humidity effects on optical refractive-index fluctuations, *Bound.-Layer Meteorology*. 20:101–109.
[32] Dole, J., R.Wilson. 2001.Turbulence Dissipation Rates and Vertical Diffusivity in the Stratosphere from Radar Observations. *Phys. Chem. Earth (B).* 26:225-229.